

Analysis of Laser-Driven Particle Acceleration from Planar Infinite Conductive Boundaries^{*}

T. Plettner

E.L. Ginzton Laboratories, Stanford University, Stanford, CA 94305

Abstract

This article explores the energy gain for a single relativistic electron from a monochromatic linearly polarized plane wave incident on a planar reflective boundary oriented at an arbitrary oblique angle, and compares the prediction for the energy gain from Inverse Transition Radiation method and the electric field path integral method. It is found that both methods predict the same energy gain regardless of the orientation of the boundary. A brief analysis on partially reflecting surfaces is presented.

^{*} work supported by Department of Energy grant DE-FG03-97ER41276

I. Introduction

The question of laser driven particle acceleration as an inverse radiation process presents an interesting view of the underlying physics for charged particle acceleration. The conservation of electromagnetic energy statement known as Poynting's Theorem [1] is the center of the inverse-radiation picture. In the case of structure based linear particle acceleration the Inverse Transition Radiation (ITR) picture predicts an energy gain equal to the overlap integral of laser and the particle's wake field radiation patterns in the far-field [2,3].

Historically the energy gain calculations for laser-driven particle acceleration in semi-open structures typically utilized the field Path Integral Method (PIM) of the incident laser field co-propagating with the electron beam and made no assumptions about the accelerator structure other than its ability to 'magically' terminate the laser field [4,5]. At first glance this raises the question to the general validity of the path integral energy gain method and would prompt us to seek special instances where we would expect ITR and PIM have different energy gain predictions.

One such candidate situation for potential differences between ITR and PIM came up in the proof-of-principle experiment (the LEAP experiment [6]) for laser-driven particle acceleration in a semi-infinite vacuum. A large fluctuation in the observed energy modulation was observed even at conditions where there appeared to be good spatial and temporal overlap between the laser and the electron beam. As a possible explanation it was hypothesized that the energy gain fluctuation was caused by shot-to-shot variations of the orientation the reflective boundary, resulting overlap variations between the laser and the transition radiation fields. The data shown in Figure 1 is an example of the fluctuation of the energy modulation typically observed.

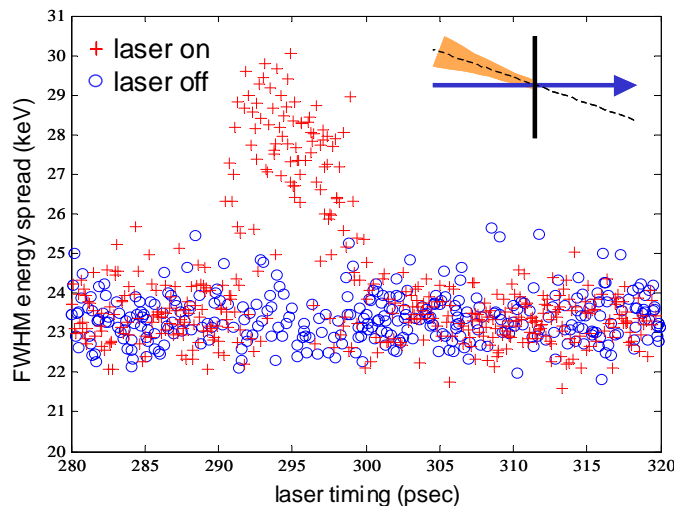


Figure 1

If the energy gain predicted by the ITR process does indeed differ from the energy gain predicted by the electric field path integral method for boundaries at oblique orientations

we would have the possibility to test this with our experimental setup, and in a future set of experiments at E163 we plan to measure the energy gain as a function of a controlled obliquity angle of the reflective tape, ranging from normal incidence to at least 45 degrees. Therefore a thorough analysis of the predictions from the ITR and the PIM pictures prior to the experiment are of interest.

II. Energy gain calculations and assumptions

We have to calculate the expected energy gain with a boundary at oblique orientation by both methods. To do this we will make the following assumptions:

- For the sake of simplicity assume that the laser beam is monochromatic and that it can be described by a plane wave. For the large gaussian laser beam we employ in the LEAP experiment this is a very good approximation. This does not compromise the physics, since we can describe laser beams of arbitrary spatial and temporal profiles as superposition of monochromatic plane waves, and the analysis for both ITR and PIM is linear.
- The boundary is a perfect high reflector. For the metallic surface of the boundary and the NIR laser this is a fairly good approximation. Absorption effects will be dealt in a subsequent article.
- The electron trajectory is straight and is unaffected by the laser or the boundary, and furthermore the electron's velocity $v=\beta c$ remains unchanged; an assumption typically made in all path integral energy gain calculations.
- The energy lost from transition radiation can be neglected.

We first evaluate the energy gain expected from the ITR picture and then proceed with the PIM picture.

III. Energy gain from the ITR picture

With the assumptions listed earlier we can utilize Poynting's Theorem and find that the energy gain of the charged particle is

$$\Delta U = \int_c \vec{E} \cdot d\vec{r} = -\frac{1}{\mu_0} \int_{-\infty}^{\infty} \oint_S (\vec{E} \times \vec{B}) \cdot \hat{n} ds dt \quad 1$$

where \vec{E} is the total electric field and \vec{B} is the total magnetic field. The total field is the superposition of the laser field and the retarded field of the charged particle. c denotes the path of the charged particle and S is the surface of the volume which encompasses the interaction. In the far field the "accelerating" E- and B-components (\vec{E}_{TR} and \vec{B}_{TR}) of the retarded fields dominate. These are normal to \hat{n} and normal to each other, that is, $\vec{E}_{TR} \perp \vec{B}_{TR} \perp \hat{n}$. The laser field can be described by an incident component $\vec{E}_I \times \vec{B}_I \propto -\hat{n}$ with flux entering S and a reflected component $\vec{E}_R \times \vec{B}_R \propto +\hat{n}$ leaving the surface S . See figure 2.

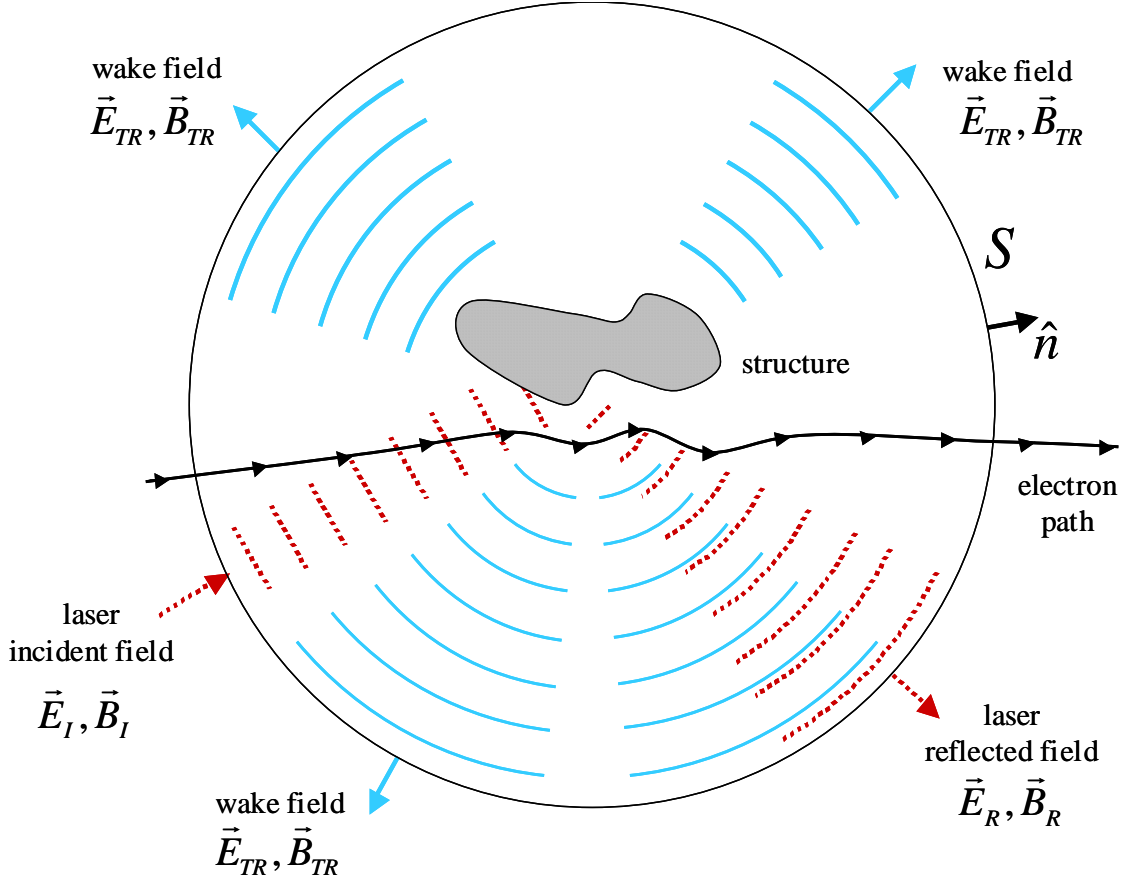


Figure 2

Using the Fourier transformation pair that has the form

$$\tilde{\vec{E}}(\vec{r}, \omega) = \int_{-\infty}^{\infty} \vec{E}(r, t) e^{-i\omega t} dt \leftrightarrow \vec{E}(r, t) = \frac{1}{2\pi} \int_{-\infty}^{\infty} \tilde{\vec{E}}(r, \omega) e^{i\omega t} d\omega \quad 2$$

and the relation between the incident, the reflected laser fields and the retarded fields we can express the energy gain of the particle of equation 1 as

$$\Delta U = -\frac{1}{\pi Z_0} \int \oint (\vec{E}_R(\omega) \cdot \vec{E}_{TR}^*(\omega)) ds d\omega \quad 3$$

where Z_0 is the vacuum impedance. A detailed derivation of equation 3 is given in the appendix. As seen in equation 3 only the reflected laser field component contributes to the overlap integral in the ITR picture. Now we need to find $\vec{E}_{TR}(\omega)$. The transition radiation from a flat infinite reflective boundary can be conveniently found by the method of image charges. We assume a charge q_1 with velocity $\vec{\beta}_1$ (normalized to c) is

incident on a flat boundary at an oblique angle. By the method of image charges there is a corresponding image charge q_2 with velocity $\vec{\beta}_2$ behind the boundary. These intersect at the boundary and can be thought of coming to a sudden stop, effectively canceling each other.

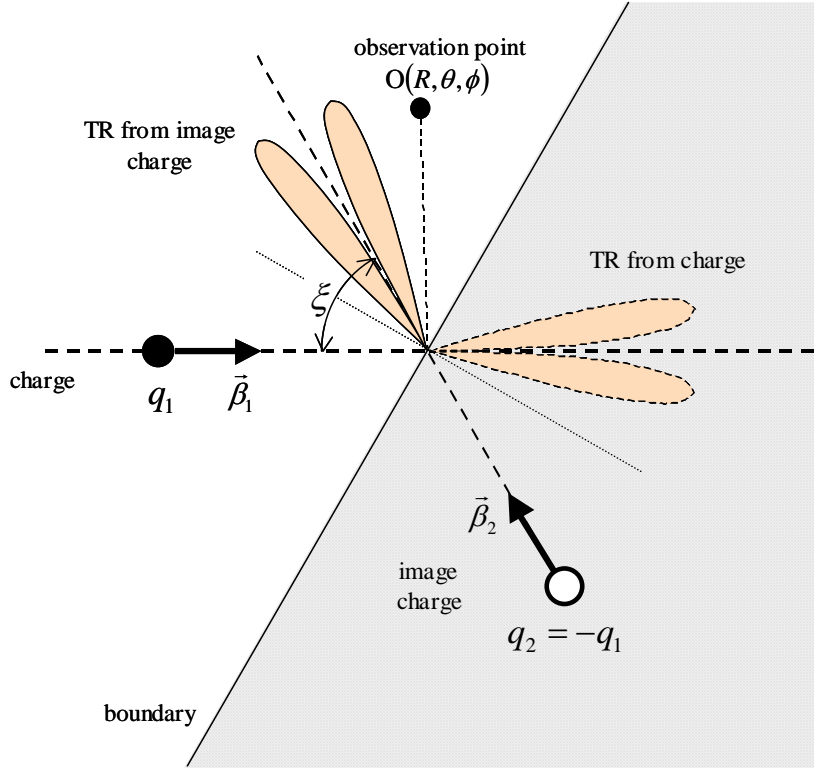


Figure 3

Starting from the retarded scalar and vector potentials for a point charge

$$\vec{A}_{ret}(\vec{x}, t) = \frac{\mu_0 q}{4\pi} \int_{-\infty}^{\infty} \frac{\vec{v} \delta(t' - t + R/c)}{R(\vec{x}, t; t')} dt' \quad 4$$

$$\Phi_{ret}(\vec{x}, t) = \frac{q}{4\pi\epsilon_0} \int_V \frac{\delta(t' - t + R/c)}{R(\vec{x}, t; t')} dt'$$

and using the electric and magnetic field expressions

$$\vec{B} = \nabla \times \vec{A}, \quad \vec{E} = -\nabla\Phi - \frac{d}{dt} \vec{A} \quad 5$$

The retarded electric field of an accelerating charge can be found to be

$$\vec{E}_{rad} = \frac{qZ_0}{4\pi KR} \frac{d}{dt'} \left(\frac{\hat{n} \times (\hat{n} \times \vec{\beta})}{K} \right) \quad 6$$

In the frequency spectrum this corresponds to

$$\vec{E}(\vec{x}, \omega) = \frac{qZ_0}{4\pi R} \int_{-\infty}^{\infty} \hat{n} \times \frac{d}{dt'} \left(\frac{\hat{n} \times \vec{\beta}}{K} \right) e^{-i\omega(t'-R/c)} dt' \quad 7$$

Assume the deceleration time for the charge q_1 is infinitely short, hence the term $e^{-i\omega(t'-R/c)}$ is approximately constant over the integration time where β changes value.

$$\vec{E}(\vec{x}, \omega) \sim \frac{qZ_0}{4\pi R} \int_{-\infty}^{\infty} \hat{n} \times \frac{d}{dt'} \left(\frac{\hat{n} \times \vec{\beta}}{K} \right) e^{i\omega R/c} dt' \sim \frac{qZ_0 e^{i\omega R/c}}{4\pi} \hat{n} \times \frac{\vec{\beta}}{K} \Bigg|_{\vec{\beta}_{initial}}^{\vec{\beta}_{final}} \quad 8$$

using $\vec{\beta}_{final} = 0$ and $\vec{\beta}_1 = \vec{\beta}_{initial} = \beta \hat{z}$ we get

$$\vec{E}_{TR,1}(R, \theta, \phi, \omega) = -\frac{q_1 Z_0}{4\pi R} \frac{\beta \sin \theta}{1 - \beta \cos \theta} \begin{pmatrix} \cos \theta \cos \phi \\ \cos \theta \sin \phi \\ -\sin \theta \end{pmatrix} e^{i\omega R/c} \quad 9$$

note that the electric field is radially polarized

$$\hat{n} \times (\hat{n} \times \vec{\beta}) = \begin{pmatrix} \cos \theta \cos \phi \\ \cos \theta \sin \phi \\ -\sin \theta \end{pmatrix} \quad 10$$

For the image charge q_2 we perform exactly the same type of calculation, except that it is convenient to introduce a separate rotated set of coordinates aligned with the initial trajectory of this charge $\hat{z}' // \vec{\beta}_2$.

$$\vec{E}_{TR,2}(R', \theta', \phi', \omega) = -\frac{q_2 Z_0}{4\pi R} \frac{\beta \sin \theta'}{1 - \beta \cos \theta'} \begin{pmatrix} \cos \theta' \cos \phi' \\ \cos \theta' \sin \phi' \\ -\sin \theta' \end{pmatrix} e^{i\omega R'/c} \quad 11$$

It is easy to verify that the cartesian coordinates (x', y', z') are related to (x, y, z) by the rotation matrix with a rotation angle of $\pi - \xi$ about \hat{y} .

$$\begin{aligned} x' &= -x \cos \xi - z \sin \xi \\ y' &= y \\ z' &= -z \cos \xi + x \sin \xi \end{aligned} \quad 12$$

and

$$\begin{aligned}
R &= \sqrt{x^2 + y^2 + z^2}, \tan \theta = \sqrt{x^2 + y^2}/z, \tan \phi = y/x \\
R' &= \sqrt{x'^2 + y'^2 + z'^2}, \tan \theta' = \sqrt{x'^2 + y'^2}/z', \tan \phi' = y'/x' \\
R' &= R
\end{aligned} \tag{13}$$

The total field is $\vec{E}_{TR} = \vec{E}_{TR,1} + \vec{E}_{TR,2}$. In our case we are interested in the TR field pattern in the xz plane ($y=0$). This allows us to express the field pattern as a function of θ . Using $q_2 = -q_1$ we obtain

$$\vec{E}_{TR} = -\frac{qZ_0 e^{i\omega R/c}}{4\pi R} \left(\frac{\beta \sin \theta'}{1 - \beta \cos \theta'} + \frac{\beta \sin \theta}{1 - \beta \cos \theta} \right) \begin{pmatrix} \cos \theta \\ 0 \\ -\sin \theta \end{pmatrix} \tag{14}$$

where $\theta' = (\pi - \xi - \theta)$

Solution in the relativistic limit

In the relativistic limit the overlap between the TR cones of the charge and the image charge are negligibly small. Since the TR cone of the charge lies in the forward direction (behind the boundary) the laser has virtually no overlap and we can approximate the TR field in the vacuum space as the contribution from the image charge

$$\vec{E}_{TR}(R', \theta') = \frac{qZ_0 e^{i\omega R'/c}}{4\pi R'} \frac{\beta \sin \theta'}{1 - \beta \cos \theta'} \begin{pmatrix} \cos \theta(\theta') \\ 0 \\ -\sin \theta(\theta') \end{pmatrix} \tag{15}$$

Next, we need to express the reflected laser field in terms of the (R', θ') coordinates. As shown in Figure 4 assume that the incident laser beam is a monochromatic plane wave at a shallow angle α with respect to the electron beam. Hence the laser field reflected from the screen $f(x', y', z')$ is propagating at a shallow angle to the \hat{z}' axis. In this instance the far-field pattern ($R' \rightarrow \infty$) of the laser beam can be expressed in terms of the Fraunhofer diffraction of the laser field at $z' = 0$.

$$f(x', y') = \frac{-ik e^{ikR'}}{2\pi R'} \int_{-\infty}^{\infty} \int_{-\infty}^{\infty} f(u, v) e^{-ik \frac{ux'}{R'} - ik \frac{vy'}{R'}} dudv \tag{16}$$

The (u, v) plane is orthogonal to the \hat{z}' axis and goes through the origin $z' = 0$. Note that $k = \omega/c$ and can be positive or negative. So when evaluating the integral of equation 16 we have to watch the sign of ω , especially when we take the absolute value of k and express it in terms of the wavelength λ .

If the boundary is a flat perfect reflector the reflected laser beam is also a plane wave. Assume that the plane wave has the form $\vec{E}_R(\vec{r}', t) = E_0 \hat{P}_R \cos(\vec{k} \cdot \vec{r}' - \omega_0 t + \phi_R)$ with

$k_x = -k_0\alpha$, $k_y = 0$, $k_z^2 = k_0^2 - k_x^2$ and $k_0 = \omega_0/c$. The coefficient $k_x = k_0\alpha$ indicates that the plane wave is at an angle α with respect to the \hat{z}' axis. \hat{P}_R is the polarization unit vector of the plane wave.

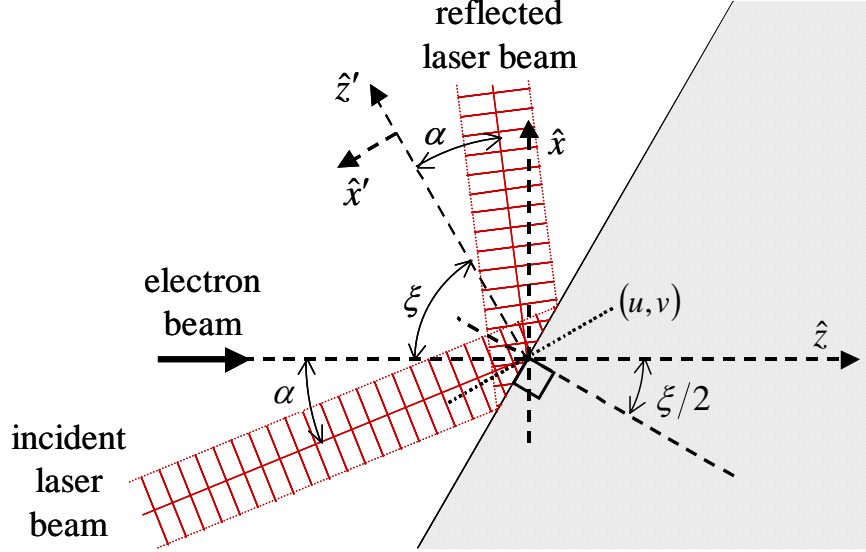


Figure 4

In the frequency domain the amplitude of the electric field is

$$E(u, v, z', \omega) = E_0 \pi \left(\delta(\omega - \omega_0) e^{i(-k_0 \alpha u + k_z z' + \varphi_R)} + \delta(\omega + \omega_0) e^{-i(-k_0 \alpha u + k_z z' + \varphi_R)} \right) \quad 17$$

Therefore the far-field diffraction amplitude is

$$f(x', y') = -\frac{i\pi k E_0 e^{ikR'}}{2\pi R'} \int_{-\infty}^{\infty} \int_{-\infty}^{\infty} \left(\delta(\omega - \omega_0) e^{i(-k_0 \alpha u + \varphi_R)} + \delta(\omega + \omega_0) e^{-i(-k_0 \alpha u + \varphi_R)} \right) e^{-iku \frac{x'}{R'} - ikv \frac{y'}{R'}} dudv \quad 18$$

(The quantity in brackets is not a vector; it is a sum.) Note that when $\omega = \omega_0 \rightarrow k = +k_0$, and when $\omega = -\omega_0 \rightarrow k = -k_0$, that is, k can be positive or negative. In equation 18 we have the integral of a complex exponential, which gives a delta function:

$$\int_{-\infty}^{\infty} e^{-ik(a+b)x} dx = (2\pi/k) \delta(a+b) \quad 19$$

$$f(x', y', \omega) = -\frac{iE_0 e^{ikR'}}{2R'} \left(\frac{2\pi}{k(\omega)} \right)^2 \delta\left(\frac{y'}{R'}\right) \left(\begin{array}{l} \delta(\omega - \omega_0) k(\omega) \delta\left(\alpha + \frac{x'}{R'} S(\omega)\right) e^{i\varphi_R} \\ + \delta(\omega + \omega_0) k(\omega) \delta\left(\alpha - \frac{x'}{R'} S(\omega)\right) e^{-i\varphi_R} \end{array} \right) \quad 20$$

where $S(\omega) = +1$ for $\omega > 0$ and $S(\omega) = -1$ for $\omega < 0$.

$$f(x', y', \omega) = -\frac{i\lambda\pi E_0 \delta(y'/R') e^{ikR'}}{R'} \begin{pmatrix} \delta\left(\frac{x'}{R'} + \alpha\right) \delta(\omega - \omega_0) e^{i\varphi_R} \\ -\delta\left(\alpha + \frac{x'}{R'}\right) \delta(\omega + \omega_0) e^{-i\varphi_R} \end{pmatrix} \quad 21$$

which simplifies to

$$f(x', y', \omega) = -\frac{2\pi\lambda E_0}{R'} \delta\left(\frac{y'}{R'}\right) \delta\left(\frac{x'}{R'} + \alpha\right) \frac{i}{2} \begin{pmatrix} \delta(\omega - \omega_0) e^{i(kR' + \varphi_R)} \\ -\delta(\omega + \omega_0) e^{i(kR' - \varphi_R)} \end{pmatrix} \quad 22$$

In the small angle approximation the coordinates θ', ϕ' are related to $x'/R', y'/R'$ by

$$\begin{aligned} \theta' &= \sqrt{x'^2 + y'^2} / R' \\ \tan \phi' &= x' / y' \end{aligned} \quad 23$$

since $\delta(u - a)\delta(v) = \delta(\theta' - a)\delta(\phi') / \sin \theta'$ (switching to spherical coordinates)

$$f(\theta', \phi', \omega) = -\frac{2\pi\lambda E_0}{R'} \frac{\delta(\pi - \phi')\delta(\alpha - \theta')}{\sin \theta'} \frac{i}{2} \begin{pmatrix} \delta(\omega - \omega_0) e^{i(kR' + \varphi_R)} \\ -\delta(\omega + \omega_0) e^{i(kR' - \varphi_R)} \end{pmatrix} \quad 24$$

The reflected laser electric field vector is

$$\begin{aligned} E_R(\theta', \phi', \omega) &= f(\theta', \phi', \omega) \hat{P}_R \\ &= -\frac{2\pi\lambda E_0}{R'} \frac{\delta(\pi - \phi')\delta(\alpha - \theta')}{\sin \theta'} \frac{i}{2} \begin{pmatrix} \delta(\omega - \omega_0) e^{i(kR' + \varphi_R)} \\ -\delta(\omega + \omega_0) e^{i(kR' - \varphi_R)} \end{pmatrix} \hat{P}_R \end{aligned} \quad 25$$

With the overlap integral of the TR field and the reflected laser beam we can evaluate the energy gain ΔU

$$\begin{aligned} \Delta U &= -\frac{1}{\pi Z_0} \int_{-\infty}^{\infty} \oint \left(\vec{E}_R(\omega) \cdot \vec{E}_{TR}^*(\omega) \right) R'^2 \sin \theta' d\theta' d\phi' d\omega \\ &= \frac{1}{\pi Z_0} \frac{qZ_0}{4\pi} \frac{2\pi E_0 \lambda}{1} \frac{i}{2} \int_{-\infty}^{\infty} \left(\delta(\omega + \omega_0) e^{i(kR' + \varphi_R)} + \delta(\omega - \omega_0) e^{i(kR' - \varphi_R)} \right) e^{-i\omega R'/c} d\omega \\ &\quad \times \oint_{\Omega} \frac{\delta(\pi - \phi')\delta(\alpha - \theta')}{\sin \theta' (1 - \beta \cos \theta')} \hat{P}_R \cdot \hat{P}_{TR} \sin^2 \theta' d\theta' d\phi \end{aligned} \quad 26$$

at $y = 0 \rightarrow \phi' = 0, \pi$ $\hat{P}_{TR} \cdot \hat{P}_R = \begin{pmatrix} \cos \theta(\theta') \\ 0 \\ -\sin \theta(\theta') \end{pmatrix} \begin{pmatrix} \cos \theta(\theta') \cos \rho \\ \sin \rho \\ -\sin \theta(\theta') \cos \rho \end{pmatrix} = \cos \rho$. Since $k = \omega/c$

$$\Delta U = \frac{qE_0 \lambda}{2\pi} \frac{i}{2} (e^{i\varphi_R} - e^{-i\varphi_R}) \frac{\beta \sin \alpha}{1 - \beta \cos \alpha} \cos \rho \quad 27$$

where $\chi = \omega_0 R'/c$ is a relative phase angle of the transition radiation at frequency ω_0 .

$$\Delta U = -\frac{qE_0 \lambda \sin \alpha}{2\pi} \frac{\beta \cos \rho \sin \varphi_R}{1 - \beta \cos \alpha} \quad 28$$

In the small angle approximation we can use $\sin \alpha \sim \alpha$, $\cos \alpha \sim 1 - \frac{1}{2}\alpha^2$, and in the relativistic limit we can approximate $\beta \sim 1 - 1/2\gamma^2$. Therefore

$$\Delta U = -\frac{qE_0 \lambda}{\pi} \frac{\alpha}{\alpha^2 + 1/\gamma^2} \cos \rho \sin \varphi_R \quad 29$$

As expected, ΔU is proportional to E_0 and λ , depends on the polarization angle ρ and on the optical phase φ_R and shows the expected dependence on the laser crossing angle $F(\alpha) = \alpha/(\alpha^2 + 1/\gamma^2)$ that has a maximum at $\alpha_{\max} = \pm 1/\gamma$.

IV. Energy gain from the path integral method, relativistic limit

For a plane wave at an angle α with respect to the electron beam describe the electric field of the incident laser beam by

$$\vec{E}_I(\vec{r}, t) = E_0 \hat{P}_I \cos(\vec{k} \cdot \vec{r} - \omega_0 t + \varphi_I) \quad 30$$

where $k_x = k_0 \alpha$, $k_y = 0$, $k_z^2 = k_0^2 - k_x^2$ and $k_0 = \omega_0/c$. Allowing for the polarization angle ρ , the polarization vector of the laser field is

$$\hat{P}_I = \begin{pmatrix} \cos \alpha \cos \rho \\ \sin \rho \\ \sin \alpha \cos \rho \end{pmatrix} \quad 31$$

Along the electron beam trajectory $(z, 0, 0, t)$ the electric field is

$$\begin{aligned}\vec{E}_I(z,0,0,t) &= E_0 \hat{P}_I \cos(k_z z - \omega_0 t + \varphi_I) \\ &= E_0 \hat{P}_I \cos(k \cos \alpha \cdot z - \omega_0 t + \varphi_I)\end{aligned}\quad 32$$

Assuming constant velocity t can be eliminated by $t = z/c\beta$. Therefore

$$\begin{aligned}\vec{E}_I(z,0,0,t) &= E_0 \hat{P}_I \cos((k \cos \alpha - \omega_0/c\beta)z + \varphi_I) \\ &= E_0 \hat{P}_I \cos((\cos \alpha - 1/\beta)kz + \varphi_I)\end{aligned}\quad 33$$

The energy gain is

$$\Delta U = q \int_c \vec{E} \cdot d\vec{r} = q \int_{-\infty}^0 (\vec{E}_I + \vec{E}_R) \cdot \hat{z} dz \quad 34$$

For now assume that electron beam is relativistic and hence the slippage distance for the reflected laser beam is very small compared to the slippage distance of the incident laser beam and therefore contribution to ΔU from the reflected laser beam is small compared to the contribution from the incident laser beam. Then

$$\Delta U = q \int_{-\infty}^0 \vec{E}_I \cdot \hat{z} dz = q \int_{-\infty}^0 E_0 \cos((\cos \alpha - 1/\beta)kz + \varphi_I) \hat{P}_I \cdot \hat{z} dz \quad 35$$

$\hat{P}_I \cdot \hat{z} = -\sin \alpha \cos \rho \sim \alpha \cos \rho$ for small angles α , and therefore

$$\Delta U = -q\alpha \cos \rho E_0 \int_{-\infty}^0 \cos((\cos \alpha - 1/\beta)kz + \varphi_I) dz \quad 36$$

The integral is of the form

$$I = \int_0^\infty \cos(u + \phi) du = \lim_{v \rightarrow 0} \int_0^\infty e^{-uv} \cos(u + \phi) du = \sin \phi \quad 37$$

Therefore the energy gain of the charged particle is

$$\begin{aligned}\Delta U &= -q\alpha \cos \rho E_0 \frac{\lambda/\pi}{\alpha^2 + \gamma^2} \int_0^\infty \cos(u - \varphi_I) du = \alpha q \cos \rho E_0 \frac{\lambda/\pi}{\alpha^2 + \gamma^2} \sin \varphi_I \\ &= \frac{qE_0 \lambda}{\pi} \frac{\alpha}{\alpha^2 + \gamma^2} \cos \rho \sin \varphi_I\end{aligned}\quad 38$$

Note that since $\varphi_l = \varphi_r + \pi$ from the Fresnel condition of reflection from a metallic surface equation 29 and equation 38 are identical, illustrating the equivalence between the ITR and the PIM pictures, at least in the highly relativistic limit.

So what about the energy gain predictions of these two methods in the low energy limit? The assumptions listed in the introduction do not make any statement about the particle's velocities, and hence we should expect the ITR and the PIM methods to give identical energy gain predictions.

V. General Solution including the low energy limit

In the low energy limit the previous assumptions for high γ break down. In the PIM picture we cannot neglect the energy gain contribution from the counter propagating laser beam, and in the ITR picture we have to include the retarded fields of both charge and image charge.

The ITR picture

The TR fields for the charge and image charge start to have significant overlap and the contribution from both has to be included for the total transition radiation field in equation 14. We had found that the transition radiation pattern had the form

$$\vec{E}_{TR}(R, \theta) = -\frac{qZ_0 e^{i\omega R/c}}{4\pi R} \left(\frac{\beta \sin(\pi - \xi - \theta)}{1 - \beta \cos(\pi - \xi - \theta)} + \frac{\beta \sin \theta}{1 - \beta \cos \theta} \right) \begin{pmatrix} \cos \theta \\ 0 \\ -\sin \theta \end{pmatrix} \quad 39$$

The two terms in the brackets represent the angular distribution functions of the retarded fields of the charge and image charge. At lower γ the denominators of these two terms do not approach zero at a particular angle and hence the radiation patterns do not form sharp and large-value peaks but start to have significant overlap at all angles. This results in a more pronounced asymmetry in the observed transition radiation cones Figure 5 shows a polar plot of the intensity of the angular distribution of the transition radiation field of equation 39, $|I_{TR}(R, \theta)/I_{\max}|$ at four different beam energies: 0.1, 2, 10 and 50 MeV.

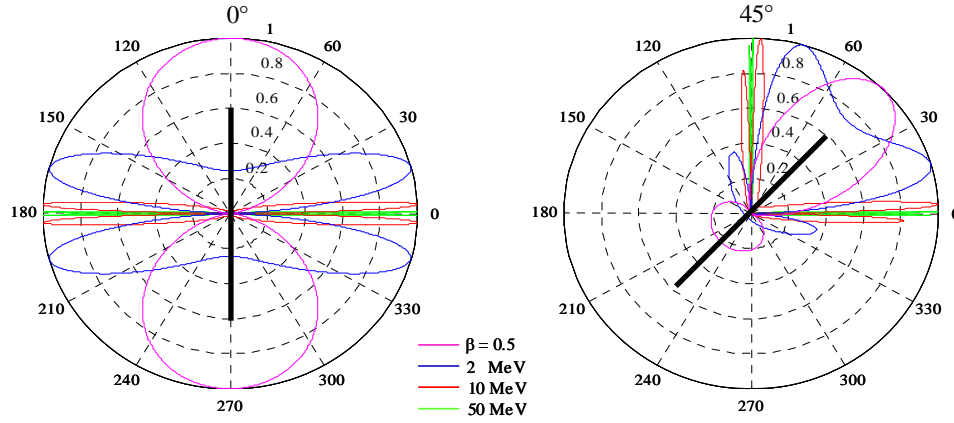


Figure 5; polar plots of $|I_{TR}(R, \theta)/I_{\max}|$ for a metal foil at normal incidence (0°), and a metal foil at 45°

It can be seen that at the lower energies the TR distribution has a wider angular spread and hence the cone asymmetry for the oblique angle surfaces is more pronounced. Hence, for reflective surfaces at oblique angles we expect an asymmetry of the energy gain depending with which side of the TR cone the reflected laser beam overlaps. Equation 39 describes the TR pattern. To calculate the overlap integral we need to express the far-field laser pattern given in terms of x', y' in equation 22 in terms of θ .

$$\vec{E}_R(\theta, \phi, R, \omega) = -\frac{2\pi\lambda E_0}{R} \frac{\delta(\pi - \xi - \theta - \alpha)\delta(\phi)}{\sin \theta} \frac{i}{2} \begin{pmatrix} \delta(\omega - \omega_0) e^{i(kR' + \varphi_R)} \\ -\delta(\omega + \omega_0) e^{i(kR' - \varphi_R)} \end{pmatrix} \hat{P}_R(\theta) \quad 40$$

$$\text{where } \hat{P}_R(\theta) = \begin{pmatrix} \cos \theta \cos \rho \\ \sin \rho \\ -\sin \theta \cos \rho \end{pmatrix}$$

Hence the energy gain from the overlap integral is

$$\begin{aligned} \Delta U &= -\frac{1}{\pi Z_0} \int_{-\infty}^{\infty} \int \int (\vec{E}_R(\omega) \cdot \vec{E}_{TR}^*(\omega)) R^2 \sin \theta d\theta d\phi d\omega \\ \Delta U &= \frac{-1}{\pi Z_0} \frac{2\pi\lambda E_0}{R} \frac{qZ_0}{4\pi R} R^2 \frac{i}{2} \int_{-\infty}^{\infty} (\delta(\omega + \omega_0) e^{i\varphi_R} + \delta(\omega - \omega_0) e^{i\varphi_R}) d\omega \\ &\quad \times \int_{\Omega} \left(\frac{\beta \sin(\pi - \xi - \theta)}{1 - \beta \cos(\pi - \xi - \theta)} + \frac{\beta \sin \theta}{1 - \beta \cos \theta} \right) \frac{\delta(\pi - \xi - \theta, \phi)}{\sin \theta} \hat{P}_R \hat{P}_{TR} \sin \theta d\Omega \end{aligned}$$

$$\Delta U = \frac{-\lambda q E_0 \sin \varphi_l}{2\pi} \left(\frac{\beta \sin \alpha}{1 - \beta \cos \alpha} + \frac{\beta \sin(\pi - \xi - \alpha)}{1 - \beta \cos(\pi - \xi - \alpha)} \right) \begin{pmatrix} \cos \theta \\ 0 \\ -\sin \theta \end{pmatrix} \begin{pmatrix} \cos \theta \cos \rho \\ \sin \rho \\ -\sin \theta \cos \rho \end{pmatrix}$$

$$\Delta U = -\frac{\lambda q E_0 \sin \varphi_l}{2\pi} \left(\frac{\beta \sin \alpha}{1 - \beta \cos \alpha} + \frac{\beta \sin(\xi + \alpha)}{1 + \beta \cos(\xi + \alpha)} \right) \cos \rho$$

$$\Delta U = -\frac{\lambda q E_0 \sin \varphi_l}{2\pi} \left(\frac{\sin \alpha}{1/\beta - \cos \alpha} + \frac{\sin(\xi + \alpha)}{1/\beta + \cos(\xi + \alpha)} \right) \cos \rho$$

I will rewrite this expression as

$$\Delta U = \frac{\lambda q E_0 \sin \varphi_l \cos \rho}{2\pi} \left(\frac{\sin \alpha}{\cos \alpha - 1/\beta} - \frac{\sin(\xi + \alpha)}{\cos(\xi + \alpha) + 1/\beta} \right) \equiv A \cdot F(\alpha, \xi; \beta) \quad 41$$

Where $F(\alpha, \xi; \beta)$ is the angular dependence function of the energy gain.

The PIM picture

Can the PIM method account for the same predicted asymmetry of the energy gain as a function of laser crossing angle? As stated earlier at lower γ the assumption that $Z_l \gg Z_R$ no longer holds: the slippage distance of the forward going laser beam Z_l reduces in length to a few λ and the contribution from the reflected laser beam becomes significant and in this limit both incident and reflected laser beam have to be taken into account.

The electric fields from the incident and the reflected laser beam were described by

$$\begin{aligned} \vec{E}_l(\vec{r}, t) &= E_0 \hat{P}_l \cos(\vec{k}_l \cdot \vec{r} - \omega_0 t + \varphi_l) \\ \vec{E}_R(\vec{r}, t) &= E_0 \hat{P}_R \cos(\vec{k}_R \cdot \vec{r} - \omega_0 t + \varphi_R) \end{aligned} \quad 42$$

where \hat{P}_l and \hat{P}_R indicate the polarization states. Now we need to find the total longitudinal electric field $E_z = E_{R,z} + E_{l,z}$ at the coordinates of the particle $\vec{r} = (0, 0, z)$.

$$\begin{aligned} E_{l,z}(0, 0, z, t) &= P_{l,z} E_0 \cos(k_{l,z} z - \omega_0 t + \varphi_l) \\ E_{R,z}(0, 0, z, t) &= P_{R,z} E_0 \cos(k_{R,z} z - \omega_0 t + \varphi_R) \end{aligned} \quad 43$$

the quantities $P_{l,z}$, $P_{R,z}$, $k_{l,z}$ and $k_{R,z}$ can be found from the figure below

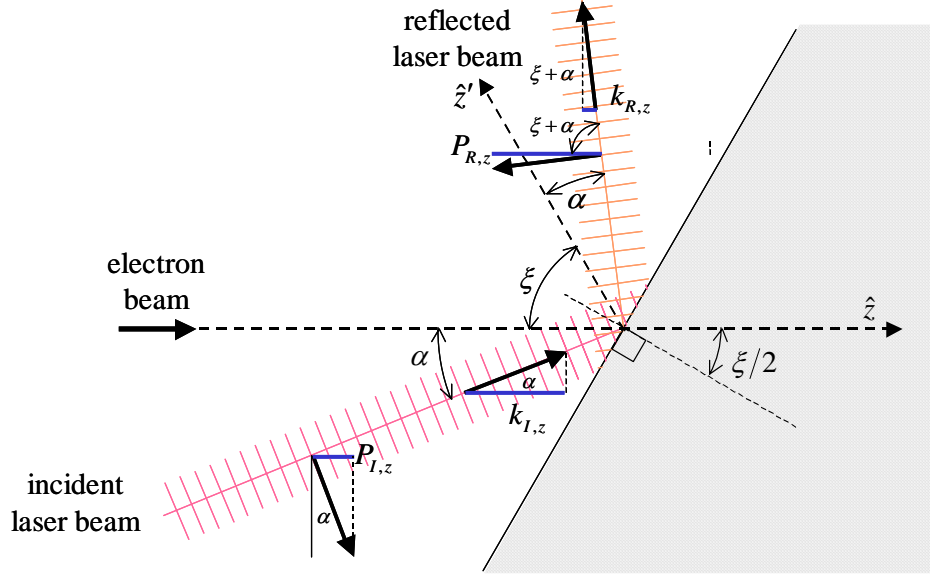


Figure 6

$$\begin{aligned}
 P_{I,z} &= \sin \alpha \cos \rho \\
 P_{R,z} &= -\sin(\alpha + \xi) \cos \rho \\
 k_{I,z} &= k \cos \alpha \\
 k_{R,z} &= -k \cos(\alpha + \xi)
 \end{aligned}
 \tag{44}$$

hence the energy gain from the incident and reflected beam is

$$\begin{aligned}
 U_I &= qE_0 \sin \alpha \cos \rho \int_{-\infty}^0 \cos(k \cos \alpha z - \omega_0 t + \varphi_I) dz \\
 U_R &= -qE_0 \sin(\xi + \alpha) \cos \rho \int_{-\infty}^0 \cos(-k \cos(\xi + \alpha) z - \omega_0 t + \varphi_R) dz
 \end{aligned}
 \tag{45}$$

Since $\varphi_I = \varphi_R + \pi$ (reflection from a metallic boundary) and $t = z/c\beta$

$$\begin{aligned}
 U_I &= qE_0 \sin \alpha \cos \rho \int_{-\infty}^0 \cos(kz[\cos \alpha - 1/\beta] + \varphi_I) dz \\
 U_R &= -qE_0 \sin(\xi + \alpha) \cos \rho \int_{-\infty}^0 \cos(-kz[\cos(\xi + \alpha) + 1/\beta] + \varphi_I + \pi) dz
 \end{aligned}
 \tag{46}$$

Using the formula of equation 37 to evaluate the cosine-integral the values of U_I and U_R of equation 46 become

$$\begin{aligned}
 U_I &= qE_0 \sin \alpha \cos \rho \frac{1}{k(\cos \alpha - 1/\beta)} \int_{-\infty}^0 \cos(u + \varphi_I) du \\
 &= \frac{\lambda q E_0 \sin \alpha \cos \rho \sin \varphi_I}{2\pi(\cos \alpha - 1/\beta)} \\
 U_R &= qE_0 \sin(\xi + \alpha) \cos \rho \frac{1}{k(\cos(\xi + \alpha) + 1/\beta)} \int_{-\infty}^0 \cos(u - \varphi_I) du \\
 &= -\frac{qE_0 \sin(\xi + \alpha) \cos \rho \sin \varphi_I}{k(\cos(\xi + \alpha) + 1/\beta)}
 \end{aligned} \tag{47}$$

Hence the total energy gain is $\Delta U = U_I + U_R$

$$\Delta U = \frac{\lambda q E_0 \cos \rho \sin \varphi_I}{2\pi} \left(\frac{\sin \alpha}{\cos \alpha - 1/\beta} - \frac{\sin(\xi + \alpha)}{\cos(\xi + \alpha) + 1/\beta} \right) \equiv A \cdot F(\alpha, \xi; \beta) \tag{48}$$

where A and $F(\alpha, \xi; \beta)$ have the same values as the energy gain calculated by the ITR method, shown in equation 41. Clearly for surfaces at oblique orientations $\xi \neq 0$ the energy gain $|\Delta U(\alpha)| \neq |\Delta U(-\alpha)|$ is not symmetric with the laser-crossing angle.

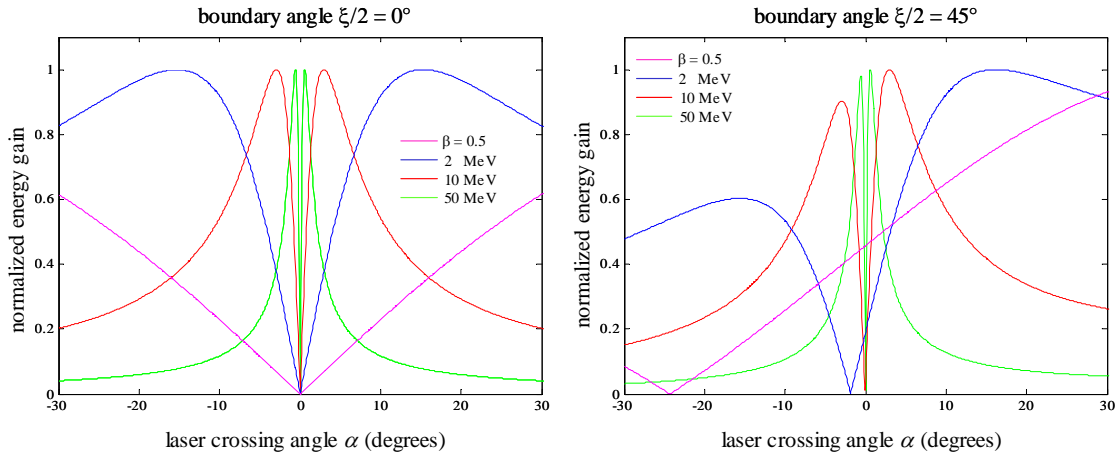


Figure 7: The angular distribution function $|F(\alpha, \xi; \beta)|/|F(\alpha_{\max}, \xi; \beta)|$ normalized to its maximum value for different beam energies

Figure 7 illustrates the normalized energy gain function for the boundary at normal incidence and at 45° . As expected, for the boundary oriented at 45° it can be observed there is a clear asymmetry of the energy gain that is more pronounced at the lower electron energies and furthermore there is a nonzero energy gain for an incident laser crossing angle of $\alpha = 0$. This is due to the electric field of the reflected laser beam being parallel to the electron trajectory and doing work for a sub-wavelength slippage distance. Although it would appear from Figure 7 that this effect is strongest at lower energies it is

actually largest for the highly relativistic case since at that limit the slippage distance approaches $\lambda/2$. A plot of $|F(\alpha, \xi; \beta)|$ versus the laser-crossing angle α shown in figure 8 illustrates this. The inset shows $|F(\alpha, \xi; \beta)|$ in the vicinity of $\alpha = 0$, and shows that at $\alpha = 0$ the function $|F(\alpha, \xi; \beta)|$ has the same small but nonzero value for the higher particle energies. Only the instance for $\beta = 0.5$ shows a significantly lower value at $\alpha = 0$, due to the reduced slippage distance at lower electron speeds.

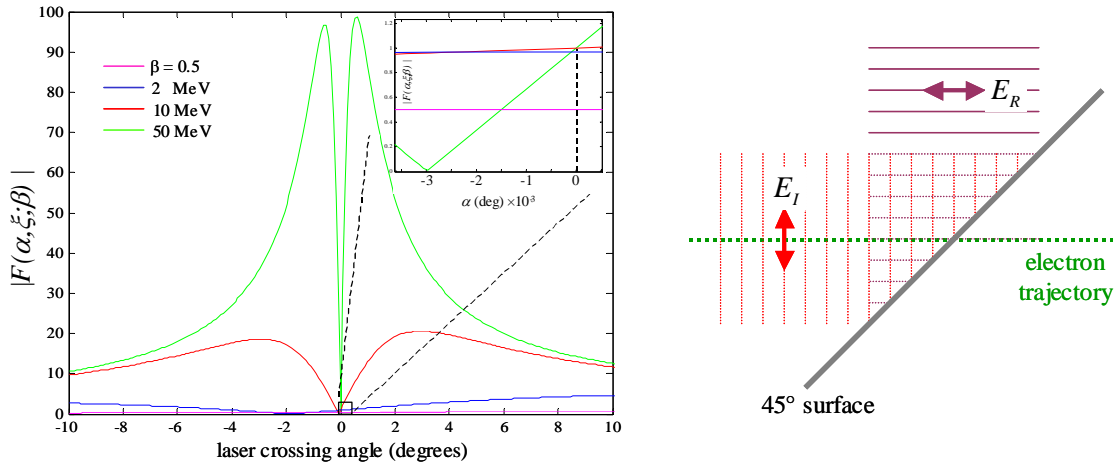


Figure 8

Let's explore this instance of having the incident laser beam at $\alpha = 0$ to the case where the high reflector surface is rotated from normal incidence $\xi = 0$ to almost at grazing incidence for the electron beam, such that the reflected laser beam slippage distance is significantly increased, or in the ITR picture the reflected laser beam is optimally overlapped with the TR pattern.

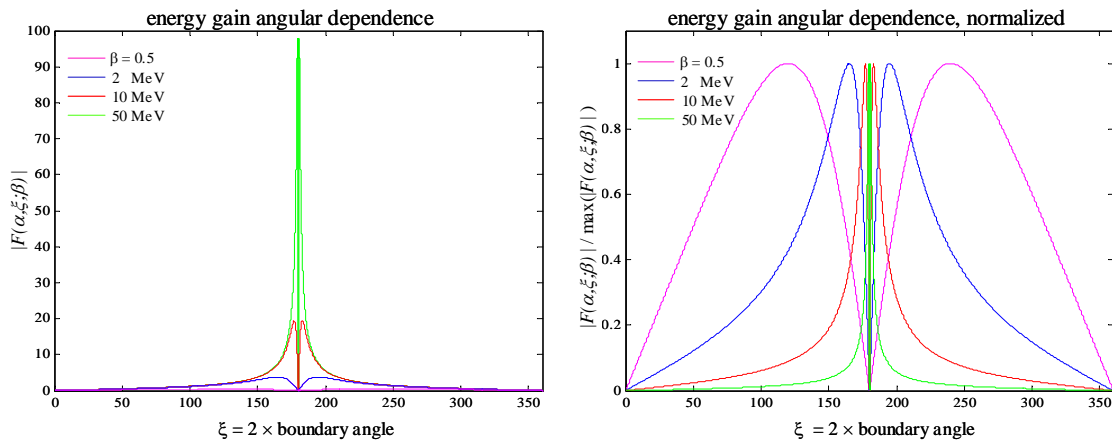


Figure 9

Figure 9 shows the function $|F(\alpha = 0, \xi; \beta)|$ as the boundary angle is swept from 0° to 180° , corresponding to sweeping the reflected laser beam from $\xi = 0^\circ$ to $\xi = 360^\circ$. As expected the optimum energy gain at higher energies occurs at very shallow angles where the reflected laser beam is almost co propagating with the electron beam and has a very long slippage distance (the optimum angle now being $|\pi - \xi| = 1/\gamma$). At the lower energies the maximum energy gain is smaller (due to the reduced slippage distance) but at the same time it is less selective to the reflected laser beam angle ξ .

It is interesting to note that the energy gain from sweeping of the angle of the reflected laser beam (either by tilting of the reflective boundary or by sweeping of the input laser beam angle is simply a probe of the transition radiation amplitude angular distribution. If the electron beam is optically bunched even the phase of the TR pattern could be determined.

VI. Laser acceleration in the downstream space of the reflective boundary

The examples involved the analysis of laser acceleration in the upstream space of a high reflector. The analysis in the downstream space is not much different, either in the ITR or in the PIM picture. The ITR energy gain equation 3 is general and also applies in this instance, and the PIM energy gain equation 34 is the same except for a change of the path integral limits to

$$\Delta U = q \int_c \vec{E} \cdot d\vec{r} = q \int_0^\infty (\vec{E}_I + \vec{E}_R) \cdot \hat{z} dz \quad 49$$

The transition radiation pattern can be found in the same fashion as before; as the particle emerges into the downstream space the fields in the downstream space can be analyzed in terms of a charge and image charge overlapped and at rest abruptly moving at a velocity βc into different directions depending on the tilt angle of the surface. Up to a phase factor this results in the same type of TR field pattern as described in equation 11.

Assume again that the input and reflected laser field is a plane wave and the tilt angle of the surface $\xi/2$ is small. The energy gain still has the same form, except that the incident laser field E_I and the reflected E_R reversed roles. Now E_R is co propagating with the electron and shows a long slippage distance while E_I is counter propagating to the electron beam and hence shows a very short slippage distance. The energy gain for laser acceleration in the downstream space is

$$\Delta U = -\frac{\lambda q E_0 \cos \rho \sin \varphi_I}{2\pi} \left(\frac{\sin(\xi + \alpha)}{\cos(\xi + \alpha) - 1/\beta} - \frac{\sin \alpha}{\cos \alpha + 1/\beta} \right) \equiv A \cdot F_R(\alpha, \xi; \beta) \quad 50$$

The main difference with the case for the acceleration upstream of the boundary is that this time the optimum occurs at $\xi + \alpha = 1/\gamma$. Also, sweeping the tilt angle of the surface or of the incident laser beam probes the amplitude of the downstream transition radiation pattern.

VII. Partially reflective boundary

As stated throughout the article the boundary was assumed to be a flat perfect reflector. We may ask how equation 50 modifies for a partially reflective surface with a reflection coefficient $r < 1$. To gain a first answer we will use the PIM picture to find the energy gain. With a less-than-perfect reflective boundary the amplitude of the reflected laser beam becomes $|E_R| = r|E_I|$ and therefore for the upstream laser acceleration we have

$$\Delta U_{upstream} = \frac{\lambda q E_0 \cos \rho \sin \varphi_I}{2\pi} \left(\frac{\sin \alpha}{\cos \alpha - 1/\beta} - r \frac{\sin(\xi + \alpha)}{\cos(\xi + \alpha) + 1/\beta} \right) \quad 51$$

and for the downstream laser acceleration we get

$$\Delta U_{downstream} = -\frac{\lambda q E_0 \cos \rho \sin \varphi_I}{2\pi} \left(r \frac{\sin(\xi + \alpha)}{\cos(\xi + \alpha) - 1/\beta} - \frac{\sin \alpha}{\cos \alpha + 1/\beta} \right) \quad 52$$

In the highly relativistic limit the counter propagating term becomes negligible and we have

$$\begin{aligned} \Delta U_{upstream} &= \frac{\lambda q E_0 \cos \rho \sin \varphi_I}{2\pi} \left(\frac{\sin \alpha}{\cos \alpha - 1/\beta} \right) \\ \Delta U_{downstream} &= -r \frac{\lambda q E_0 \cos \rho \sin \varphi_I}{2\pi} \left(\frac{\sin(\xi + \alpha)}{\cos(\xi + \alpha) - 1/\beta} \right) \end{aligned} \quad 53$$

With the PIM picture and in the highly relativistic limit we expect to see no significant effect from a poorly reflective boundary for laser acceleration in the upstream space while in the downstream space we expect $|\Delta U_{downstream}| \propto r$

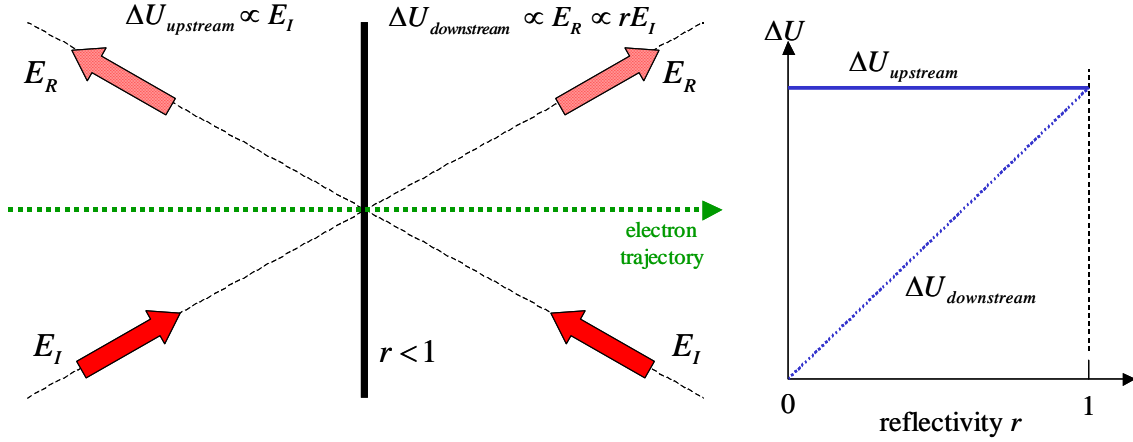


Figure 10

The ITR picture would predict a different outcome, especially for the upstream acceleration case, which from the PIM picture appears to be independent of the boundary properties. The ITR picture would expect a reduction of the energy gain due to the reduced reflected laser field component and from a reduced TR pattern from the lossy medium. The discrepancy lies in the assumptions made in the ITR picture, where the medium is assumed to have no ohmic loss and the only nonzero terms in Poynting's theorem are the electric field path integral of the traveling particle and the far-field radiative terms. With a lossy medium Poynting's Theorem would become

$$\Delta U_{particle} + \int_{\tau_M} \vec{J}_M \cdot \vec{E} dv dt = -\Delta U_{EM} - \frac{1}{\mu_0} \int_{\tau_S} \oint (\vec{E} \times \vec{B}) \cdot \hat{n} ds dt \quad 54$$

\vec{J}_M is the current inside the medium M . If the medium is lossy the external electric field penetrates the medium and $|\vec{E}| \neq 0$ inside the medium, making the volume integral of the currents and fields $\int \vec{J}_M \cdot \vec{E} dv$ in the medium M in equation 54 nonzero. If the total volume in equation 54 did not store electromagnetic energy during the transit of the particle $\Delta U_{EM} = 0$ and we would be left with

$$\Delta U_{particle} = - \int_{\tau_M} \vec{J}_M \cdot \vec{E} dv dt - \frac{1}{\mu_0} \int_{\tau_S} \oint (\vec{E} \times \vec{B}) \cdot \hat{n} ds dt \quad 55$$

Hence for a lossy medium the energy gain predicted by the inverse-radiation picture is not correct.

$$\Delta U_{particle} \neq - \frac{1}{\mu_0} \int_{\tau_S} \oint (\vec{E} \times \vec{B}) \cdot \hat{n} ds dt \quad 56$$

The inclusion of a laser-absorbing boundary is a simple extension to the planed set of experiments with reflective boundaries and will provide an experimental opportunity to both test for the failure of the ITR picture and for the validity of the PIM picture under a more general boundary condition.

VIII. Conclusions

It has been shown that for perfect reflective flat boundaries the energy gain predicted by the ITR and the PIM methods yield exactly the same value, regardless of the particle's initial energy, the orientation of the boundary, or the upstream or downstream acceleration case. Hence we can rule out the hypothesis that the observed energy fluctuations were due to random tilting of the boundary surface. A high reflector boundary of the type used in the previous proof-of-principle experiment with laser acceleration cannot distinguish between ITR and the PIM pictures. Given the perfect-reflector assumption this finding should not be surprising at all, since for lossless media Poynting's Theorem collapses to equation 1, which puts the path integral energy gain and the radiation overlap integral on an equal footing.

However, the brief analysis of the expected particle acceleration in the upstream space of lossy boundaries ($r < 1$) appears to show a case where the ITR picture clearly differs in its energy gain predictions from the PIM picture. It is argued that the ITR picture does not apply to these instances because of the appearance of an additional ohmic loss term of the material that prevents Poynting's Theorem from collapsing to the simple expression of equation 1. This brief analysis is a motivation for a more detailed treatment of a more generalized inverse-radiation picture that includes lossy materials.

Another interesting instance to be analyzed is the case of a lossless transparent boundary of the appropriate thickness that could reset the laser phase and effectively double the energy gain.

IX. Appendix

In the far field region the electric and magnetic fields have the relations $|\vec{E}_I| = c|\vec{B}_I|$, $|\vec{E}_R| = c|\vec{B}_R|$ and $|\vec{E}_{TR}| = c|\vec{B}_{TR}|$. Also, the electric and magnetic field components are mutually orthogonal and obey

$$\begin{aligned} \vec{E}_I &\perp \vec{B}_I \perp \hat{n} \\ \vec{E}_R &\perp \vec{B}_R \perp \hat{n} \\ \vec{E}_{TR} &\perp \vec{B}_{TR} \perp \hat{n} \end{aligned} \tag{A1}$$

$$\begin{aligned} \vec{E}_I \times \vec{B}_I &= 1/c |E_I|^2 (-\hat{n}) \\ \vec{E}_R \times \vec{B}_R &= 1/c |E_R|^2 \hat{n} \end{aligned} \tag{A2}$$

$$\vec{E}_{TR} \times \vec{B}_{TR} = 1/c |E_{TR}|^2 \hat{n}$$

Note that the negative term for the incident field indicates an inward flux of energy. The total electric and magnetic fields are $\vec{E} = \vec{E}_I + \vec{E}_R + \vec{E}_{TR}$ and $\vec{B} = \vec{B}_I + \vec{B}_R + \vec{B}_{TR}$. Hence the integral of equation 1 reads

$$d_t U = -\frac{1}{\mu_0} \oint_S (\vec{E} \times \vec{B}) \cdot \hat{n} ds = -\frac{1}{\mu_0} \oint_S (\vec{E}_I + \vec{E}_R + \vec{E}_{TR}) \times (\vec{B}_I + \vec{B}_R + \vec{B}_{TR}) \cdot \hat{n} ds \quad A3$$

which expands to

$$d_t U = -\frac{1}{\mu_0} \left(\begin{aligned} & \oint_S (-1/c |E_I|^2 \hat{n} + 1/c |E_R|^2 \hat{n} + 1/c |E_{TR}|^2 \hat{n}) \cdot \hat{n} ds \\ & + \oint_S (\vec{E}_I \times \vec{B}_R + \vec{E}_R \times \vec{B}_I) \cdot \hat{n} ds \\ & + \oint_S (\vec{E}_I \times \vec{B}_{TR} + \vec{E}_R \times \vec{B}_{TR} + \vec{E}_{TR} \times \vec{B}_I + \vec{E}_{TR} \times \vec{B}_R) \cdot \hat{n} ds \end{aligned} \right) \quad A4$$

For the very first surface integral in A4, if the medium is a perfect reflector the output reflected power is equal to the input incident power, regardless of the shape of the reflector, and we have

$$\oint_S (1/c |E_I|^2 \hat{n}) \cdot \hat{n} ds = \oint_S (1/c |E_R|^2 \hat{n}) \cdot \hat{n} ds \quad A5$$

and therefore the 1st surface integral reduces to the wake field radiation term

$$\oint_S (-1/c |E_I|^2 \hat{n} + 1/c |E_R|^2 \hat{n} + 1/c |E_{TR}|^2 \hat{n}) \cdot \hat{n} ds = \oint_S (1/c |E_{TR}|^2 \hat{n}) \cdot \hat{n} ds \equiv \Delta P_{TR} \quad A6$$

The second surface integral of A4 can be evaluated from the relations in A1. The cross products have the form

$$\begin{aligned} \vec{E}_I \times \vec{B}_R &= |\vec{E}_I| |\vec{B}_R| \sin \varphi \hat{n} = 1/c |\vec{E}_I| |\vec{E}_R| \cos \varphi \hat{n} = 1/c (\vec{E}_I \cdot \vec{E}_R) \hat{n} \\ \vec{E}_R \times \vec{B}_I &= -|\vec{E}_I| |\vec{B}_R| \sin \varphi \hat{n} = -1/c |\vec{E}_I| |\vec{E}_R| \cos \varphi \hat{n} = -1/c (\vec{E}_I \cdot \vec{E}_R) \hat{n} \end{aligned} \quad A7$$

The sign reversal of the second expression in A7 with respect to the first is due to the opposite flux directions of the incident and reflected fields. Now we can see that the 2nd surface integral of A4 reduces to zero.

$$\oint_S (\vec{E}_I \times \vec{B}_R + \vec{E}_R \times \vec{B}_I) \cdot \hat{n} ds = 0 \quad \text{A8}$$

For the 3rd surface integral in A4 we can find a similar set of values for the cross products

$$\begin{aligned} \vec{E}_I \times \vec{B}_{TR} &= |\vec{E}_I| |\vec{B}_{TR}| \sin \phi \hat{n} = 1/c (\vec{E}_I \cdot \vec{E}_{TR}) \hat{n} \\ \vec{E}_{TR} \times \vec{B}_I &= -|\vec{E}_I| |\vec{B}_{TR}| \sin \phi \hat{n} = -1/c (\vec{E}_I \cdot \vec{E}_{TR}) \hat{n} \\ \vec{E}_R \times \vec{B}_{TR} &= |\vec{E}_R| |\vec{B}_{TR}| \sin \phi \hat{n} = 1/c (\vec{E}_R \cdot \vec{E}_{TR}) \hat{n} \\ \vec{E}_{TR} \times \vec{B}_R &= +|\vec{E}_R| |\vec{B}_{TR}| \sin \phi \hat{n} = 1/c (\vec{E}_R \cdot \vec{E}_{TR}) \hat{n} \end{aligned} \quad \text{A9}$$

Note that for the pair of $\vec{E}_R \times \vec{B}_{TR}$ and $\vec{E}_{TR} \times \vec{B}_R$ there is no sign reversal since both reflected field and the wake field have a flux of energy in the same (outward) direction. Hence the 3rd surface integral collapses to

$$\oint_S (\vec{E}_R \times \vec{B}_{TR} + \vec{E}_{TR} \times \vec{B}_R) \cdot \hat{n} ds = 2/c \oint_S (\vec{E}_R \cdot \vec{E}_{TR}) ds \quad \text{A10}$$

Therefore the total energy gain is

$$\Delta U = -\frac{2}{\mu_0 c} \int_{-\infty}^{\infty} \oint_S (\vec{E}_R \cdot \vec{E}_{TR}) ds dt - \Delta U_{TR} \quad \text{A11}$$

Taking into account the assumptions listed in the introduction we can neglect ΔU_{TR} and are left with

$$\Delta U = -\frac{2}{Z_0} \int_{-\infty}^{\infty} \oint_S (\vec{E}_R(t) \cdot \vec{E}_{TR}(t)) ds dt \quad \text{A12}$$

With the Fourier transform definition in equation 2

$$\Delta U = -\frac{2}{Z_0} \int_{-\infty}^{\infty} \int_{-\infty}^{\infty} \int_{-\infty}^{\infty} \left(\frac{1}{2\pi} \right)^2 (\tilde{E}_R(\omega) \cdot \tilde{E}_{TR}(\omega') e^{i(\omega+\omega')t}) d\omega d\omega' ds dt \quad \text{A13}$$

which can be rearranged to

$$\begin{aligned}
\Delta U &= -\frac{2}{Z_0} \left(\frac{1}{2\pi} \right)^2 \int_{-\infty}^{\infty} \int_{-\infty}^{\infty} \int_S \tilde{E}_R(\omega) \cdot \tilde{E}_{TR}(\omega') ds \left(\int_{-\infty}^{\infty} e^{i(\omega+\omega')t} dt \right) d\omega d\omega' \\
&= -\frac{2}{Z_0} \left(\frac{1}{2\pi} \right)^2 \int_{-\infty}^{\infty} \int_{-\infty}^{\infty} \int_S \tilde{E}_R(\omega) \cdot \tilde{E}_{TR}(\omega') ds 2\pi\delta(\omega+\omega') d\omega d\omega' \\
&= -\frac{1}{\pi Z_0} \int_{-\infty}^{\infty} \int_S \tilde{E}_R(\omega) \cdot \tilde{E}_{TR}(-\omega) ds d\omega
\end{aligned} \tag{A14}$$

For real functions of time $\tilde{E}_{TR}(-\omega) = \tilde{E}_{TR}^*(\omega)$ and therefore

$$\Delta U = -\frac{1}{\pi Z_0} \int_{-\infty}^{\infty} \int_S \tilde{E}_R(\omega) \cdot \tilde{E}_{TR}^*(\omega) ds d\omega \tag{A15}$$

This proves the particle energy gain formula shown in equation 3.

X. References

1. See for example Jackson, Classical Electrodynamics, 2nd edition, chapter 6, p 236
2. M. Xie, "A Fundamental Theorem on Particle Acceleration", Proceedings of the 2003 Particle Accelerator Conference (2003)
3. Z. Huang, G. Stupakov and M. Zolotarev, "Calculation and Optimization of Laser Acceleration in Vacuum", Phys. Rev. Special Topics - Accelerators and Beams, Vol. 7, 011302 (2004)
4. J.A. Edginghofer, R.H. Pantell, "Energy exchange between free electrons and light in vacuum", Journal of Applied Physics, 50, p 6120-6122 (1979)
5. E. Esarey, P. Sprangle, J. Krall, "Laser Acceleration of Electrons in Vacuum", Physical Review E, 52, p 5443-5453 (1995)
6. T. Plettner, R.L. Byer, E. Colby, B. Cowan, C.M.S. Sears, J. E. Spencer, R.H. Siemann, "Proof-of-principle experiment for laser-driven acceleration of relativistic electrons in a semi-infinite vacuum", Phys. Rev. ST Accel. Beams 8, 121301 (2005)